

Modeling the Multi-band Light Curves of the Afterglows of Three Gamma-Ray Bursts and Their Associated Supernovae

Ji-Shun LIAN (连纪顺),¹ SHAN-QIN WANG(王善钦),¹ WEN-PEI GAN (甘文沛),¹ JING-YAO LI (李京谣),¹ AND EN-WEI LIANG (梁恩维)¹

¹Guangxi Key Laboratory for Relativistic Astrophysics, School of Physical Science and Technology, Guangxi University, Nanning 530004, China

ABSTRACT

There are some dozen supernovae (SNe) associated with long Gamma-ray bursts (GRBs) have been confirmed. Most of previous studies derive the physical properties of the GRB-SNe by fitting the constructed (psuedo-)bolometric light curves. However, many GRB-SNe have only a few filter data, for which the (psuedo-)bolometric light curves are very difficult to be constructed. Additionally, constructing (psuedo-)bolometric light curves rely on some assumptions. In this paper, we use the multi-band broken power-law plus ⁵⁶Ni model to fit the multi-band light curves of the afterglows and the SNe (SN 2001ke, SN 2013dx, and SN 2016jca) associated with three GRBs (GRB 011121, GRB 130702A, and GRB 161219B). We find our model can account for the multi-band light curves of the three GRB-SNe (except for the late-time z-band light curves of two events), indicating that the model is a reliable model. The ⁵⁶Ni masses we derive are higher than that in the literature. This might be due to the fact that the ⁵⁶Ni masses in the literature are usually obtained by fitting the psuedo-bolometric light curves whose luminosities are usually (significantly) underestimated. We suggest that the multi-band model can not only be used to fit the multi-band light curves of GRB-SNe that have many filter observations, but also fit those having sparse data.

Keywords: general – supernovae: individual (GRB 011121/SN 2001ke, GRB 130702A/SN 2013dx, GRB 161219B/SN 2016jca)

1. INTRODUCTION

Gamma-ray bursts (GRBs) are the most powerful explosions in the universe. It is widely believed that GRBs come from the relativistic jet launched by the central engine (Woosley 2011). The interactions between the jets with the surrounding medium would produce X-ray, UV-optical-NIR and radio afterglows (see Zhang 2018 and references therein). According to the observation of prompt emission duration, GRBs is divided into long-duration bursts (LGRBs) and short-duration bursts (SGRBs) with a dividing line of ~ 2 seconds (Kouveliotou et al. 1993). The observations and analysis for some dozen supernovae (SNe) associated with LGRBs (Hjorth et al. 2003; Matheson et al. 2003; Stanek et al. 2003; Malesani et al. 2004; Deng et al. 2005; Modjaz et al. 2006; Mirabal et al. 2006; Sollerman et al. 2006; Campana et al. 2006; Maeda et al. 2007; Chornock et al. 2010; Starling et al. 2011; Olivares et al. 2012; Bufano et al. 2012; Melandri et al. 2012; Singer et al. 2013; Schulze et al. 2014; Melandri et al. 2014; Toy et al. 2016; D’Elia et al. 2015; Cano et al. 2017a; Volnova et al. 2017; Ashall et al. 2019; Melandri et al. 2019; Hu et al. 2021) indicate that most LGRBs are produced by the explosions of massive stars. On the other hand, the confirmation of SSS17a/AT2017gfo which is a kilonova associated with GW170817 that is a gravitational wave emitted by a merger of a neutron star binary and GRB 170817A that is an SGRB (Arcavi et al. 2017; Shappee et al. 2017; Abbott et al. 2017; Coulter et al. 2017; Shappee et al. 2017) supports the conjecture that at least a fraction of SGRBs are produced by the mergers of compact binary stars.

The SNe associated with LGRBs are called GRB-SNe (Woosley & Bloom 2006; Hjorth et al. 2012; Cano et al. 2017b). On average, one or two GRB-SNe can be found every year. To date, there are about 60 LGRBs that have been confirmed to be associated with SNe. Almost all GRB-SNe are broad-lined Ic (Ic-BL) SNe whose optical spectra are hydrogen-deficient and show broad absorption line features. The spectral features indicate that the progenitors of GRB-SNe are highly stripped, and might be Wolf-Rayet stars (Price et al. 2002; Sonbas et al. 2008). The broad absorption lines are indicative of huge ejecta velocities $\gtrsim 2 \times 10^9$ cm s⁻¹. Therefore, a major fraction of GRB-SNe (and the SNe Ic-BL without accompanying GRBs) become

so-called ‘‘hypernovae’’ (HNe) whose kinetic energy is $\gtrsim 10^{52}$ erg, which is about 10 times that of normal SNe. The explosion mechanisms of GRB-SNe are still elusive.

The most prevailing model adopted to account for the light curves of GRB-SNe is ^{56}Ni cascade decay ($^{56}\text{Ni} \rightarrow ^{56}\text{Co} \rightarrow ^{56}\text{Fe}$) model (the ^{56}Ni model, Arnett 1979, 1980, 1982, 1996). Some very luminous GRB-SNe cannot be explained by the ^{56}Ni model, and alternative or additional energy sources (e.g., the magnetar spinning-down, the fall-back accretion, etc.) are employed to account for the light curves.

Previous studies focusing on GRB-SNe usually construct the psuedo-bolometric light curves of the SNe and derive the physical properties of GRB-SNe by fitting the constructed psuedo-bolometric light curves. It should be noted that, however, the process constructing the psuedo-bolometric light curves might underestimate the luminosities of the SNe and therefore underestimate the ^{56}Ni masses.

Recently, the model directly fit the multi-band light curves (Nicholl et al. 2017) have been adopted to fit the light curves of superluminous SNe (Nicholl et al. 2017; Moriya et al. 2018), the tidal disruption events (Mockler et al. 2019), the luminous rapidly evolving optical transients (Wang et al. 2019), and ordinary SNe Ib and Ic (Wang et al. 2022).

In this paper, we collect published data of the (UV-)optical–NIR counterparts (GRB 011121/SN 2001ke, GRB 130702A/SN 2013dx, GRB 161219B/SN 2016jca) of three GRBs (GRB 011121, GRB 130702A, GRB 161219B; here, the GRBs represent their afterglows) and use the broken power-law plus ^{56}Ni model to fit their multi-band light curves. In Section 2, we model the multi-band light curves of the three GRB-SNe using the ^{56}Ni model. In Section 3, we compare parameters and the bolometric properties of the SNe to that in the literature. We draw some conclusions in Section 4. The values of the foreground reddening of the Milky Way ($E(B - V)_{\text{MW}}$) are from Schlafly & Finkbeiner (2011). The standard cosmological parameters ($\Omega_m = 0.315$, $\Omega_\Lambda = 0.685$, and $H_0 = 67.3 \text{ kms}^{-1}\text{Mpc}^{-1}$, Planck Collaboration 2014) are adopted throughout this paper.

2. MODELING THE MULTI-BAND LIGHT CURVES OF THREE GRB-SNE USING THE ^{56}Ni MODEL

The information of the GRB 011121/SN 2001ke, GRB 130702A/SN 2013dx, GRB 161219B/SN 2016jca are list in Table 1. The flux of the host galaxy of GRB 011121/SN 2001ke is negligible, and the flux of the host galaxies of GRB 130702A/SN 2013dx and GRB 161219B/SN 2016jca have been subtracted (the magnitudes of the two host galaxies are from Volnova et al. (2017) and Laskar et al. (2018), respectively, and listed in Table 2). Then the flux of the (UV-)optical–NIR counterpart of a GRB-SN ($F_{v,\text{tot}}(t)$) can be divided into that of the GRB afterglow ($F_{v,\text{AG}}(t)$) and that of the SN ($F_{v,\text{SN}}(t)$) associated with the GRB, i.e., $F_{v,\text{tot}}(t) = F_{v,\text{AG}}(t) + F_{v,\text{SN}}(t)$.

The flux density of an afterglow is proportional to a broken power-law decay function ($F_{v,\text{AG}}(t) \propto ((t/t_b)^{\alpha_1 n} + (t/t_b)^{\alpha_2 n})^{-1/n}$, Beuermann et al. 1999, in the representation of Zeh et al. 2004) and $v^{-\beta}$ ($F_{v,\text{AG}}(t) \propto v^{-\beta}$), and can be expressed as $F_{v,\text{AG}}(t) = A_{\text{AG}} \cdot ((t/t_b)^{\alpha_1 n} + (t/t_b)^{\alpha_2 n})^{-1/n} \cdot v^{-\beta}$. The definitions of α_1 , α_2 , t_b , n , and β are presented in Table 3.

We assume that the SN associated with a GRB was powered by ^{56}Ni cascade decay. The bolometric luminosity of ^{56}Ni -powered SNe powered is (see e.g., Arnett 1982; Chatzopoulos et al. 2012; Wang et al. 2015; Wang & Gan 2022)

$$L_{\text{SN}}(t) = \frac{2}{\tau_m} e^{-\frac{t}{\tau_m}} \int_0^t e^{\frac{t'}{\tau_m}} \frac{t'}{\tau_m} \left(\epsilon_{\text{Ni}} M_{\text{Ni}} e^{-t'/\tau_{\text{Ni}}} + \epsilon_{\text{Co}} M_{\text{Ni}} \frac{e^{-t'/\tau_{\text{Co}}} - e^{-t'/\tau_{\text{Ni}}}}{1 - \tau_{\text{Ni}}/\tau_{\text{Co}}} \right) (1 - e^{-\tau_\gamma(t)}) dt', \quad (1)$$

here, $\tau_m = (2\kappa M_{\text{ej}}/\beta_{\text{SN}} v_{\text{ph}} c)^{1/2}$ is the diffusion timescale, $\tau_\gamma(t) = 3\kappa_\gamma M_{\text{ej}}/4\pi v_{\text{ph}}^2 t^2$ is the optical depth to γ -rays (Chatzopoulos et al. 2009, 2012). κ is the optical opacity of the ejecta which is set to be $0.07 \text{ cm}^2 \text{ g}^{-1}$, c is the speed of light, $\beta \simeq 13.8$ is a constant (Arnett 1982), $\epsilon_{\text{Ni}} = 3.9 \times 10^{10} \text{ erg s}^{-1} \text{ g}^{-1}$ (Sutherland & Wheeler 1984; Cappellaro et al. 1997), $\tau_{\text{Ni}} = 8.8 \text{ days}$, $\epsilon_{\text{Co}} = 6.8 \times 10^9 \text{ erg s}^{-1} \text{ g}^{-1}$ (Maeda et al. 2003), $\tau_{\text{Co}} = 111.3 \text{ days}$.

Assuming the early-time photosphere radii of the SNe is proportional to the time, and the ejecta cool to constant temperatures (T_f), the temperatures and radii can be given by (Nicholl et al. 2017):

$$T_{\text{ph}}(t) = \begin{cases} \left(\frac{L_{\text{SN}}(t)}{4\pi\sigma v_{\text{ph}}^2 t^2} \right)^{\frac{1}{4}}, & \left(\frac{L_{\text{SN}}(t)}{4\pi\sigma v_{\text{ph}}^2 t^2} \right)^{\frac{1}{4}} > T_f \\ T_f, & \left(\frac{L_{\text{SN}}(t)}{4\pi\sigma v_{\text{ph}}^2 t^2} \right)^{\frac{1}{4}} \leq T_f \end{cases} \quad (2)$$

$$R_{\text{ph}}(t) = \begin{cases} v_{\text{ph}} t, & \left(\frac{L_{\text{SN}}(t)}{4\pi\sigma v_{\text{ph}}^2 t^2} \right)^{\frac{1}{4}} > T_f \\ \left(\frac{L_{\text{SN}}(t)}{4\pi\sigma T_f^4} \right)^{\frac{1}{2}}, & \left(\frac{L_{\text{SN}}(t)}{4\pi\sigma v_{\text{ph}}^2 t^2} \right)^{\frac{1}{4}} \leq T_f \end{cases} \quad (3)$$

To fit the multi-band light curves of the SN components, we suppose that the spectral energy distributions (SEDs) of the SNe can be described by the UV absorbed blackbody model (Prajs et al. 2017; Nicholl et al. 2017),

$$F_{\nu, \text{SN}} = \begin{cases} \left(\frac{\lambda}{\lambda_{\text{CF}}}\right)(2\pi h\nu^3/c^2)(e^{\frac{h\nu}{k_b T_{\text{ph}}}} - 1)^{-1} \frac{R_{\text{ph}}^2}{D_L^2}, & \lambda \leq \lambda_{\text{CF}} \\ (2\pi h\nu^3/c^2)(e^{\frac{h\nu}{k_b T_{\text{ph}}}} - 1)^{-1} \frac{R_{\text{ph}}^2}{D_L^2}, & \lambda > \lambda_{\text{CF}} \end{cases} \quad (4)$$

here, $\lambda_{\text{CF}} = 3000 \text{ \AA}$ is the cutoff wavelength (Prajs et al. 2017; Nicholl et al. 2017).

The definitions, the units, and the priors of the parameters of the model are listed in Table 3. The values of $A_{V, \text{host}}$ (or $E(B - V)_{\text{host}}$) of GRB 130702A/SN 2013dx and GRB 161219B/SN 2016jca have been given by the literature, and can be set to be constants. Hence, the multi-band ^{56}Ni model fitting GRB 130702A/SN 2013dx and GRB 161219B/SN 2016jca has five free parameters (M_{ej} , v_{ph} , M_{Ni} , κ_{γ} , and T_{f}). GRB 011121/SN 2001ke is far away from the host galaxy (Bloom et al. 2002); Greiner et al. (2003) suggest that it has no host galaxy extinction, while Küpcü Yoldaş et al. (2007) get an upper limit of $E(B - V)_{\text{host}}$ (0.08 mag). We assume that $A_{V, \text{host}}$ of GRB 011121/SN 2001ke is an additional free parameter whose range is 0 to 0.248 mag. Additionally, we assume that the ratio of M_{Ni} to M_{ej} is ≤ 0.2 (Umeda & Nomoto 2008). We adopt the Markov Chain Monte Carlo (MCMC) method by using emcee of Python package (Foreman-Mackey et al. 2013) to fit the data to obtain the best-fitting parameters and 1σ parameter range.

The fits of the three GRB-SNe and the best-fit parameters are presented in Figure 1 and Table 4, respectively. The corresponding corner plots are shown in Figures A1, A2, and A3 in the Appendix. All or most optical and NIR bands of the three GRB-SNe can be fitted by the multi-band model, except for the late-time z -band light curve of GRB 130702A/SN 2013dx and GRB 161219B/SN 2016jca which cannot be well fitted by the multi-band model (see the top and bottom-left panels of Figure 1).

The UV band light curves cannot be well fitted by the model. As shown in Figure 2 of Laskar et al. (2018), the values of α_2 of different UV bands of GRB 161219B/SN 2016jca are different. Hence, assuming a same value of α_2 for all bands can result in a bad fit. To improve the fit, we assume that the values of α_2 in different UV bands are different from each other, and different from the value in optical and NIR bands. The new fit for the light curves of GRB 161219B/SN 2016jca and the corresponding corner plot are presented in the bottom-right panel of Figure 1 and Figure A4, respectively. The parameters of the new fit are listed in the last column of Table 4. We find that the new fit is better than the first fit since the UV bands are also well matched by the model.

There are two (possible) reasons that can explain the bad quality of the fits for z -band light curves of the two GRB-SNe. (1). Their late-time z -band light curves show fluctuation features that cannot be fully fitted by the theoretical light curves which are smooth. (2). Their late-time SEDs deviate the blackbody function in z -band.

The derived masses of ^{56}Ni of SN 2001ke, SN 2013dx and SN 2016jca are $0.46 \pm 0.01 M_{\odot}$, $0.74 \pm 0.01 M_{\odot}$, and $0.33 \pm 0.00 M_{\odot}$, respectively. The ejecta masses of the three GRB-SNe are $4.02^{+0.53}_{-0.58} M_{\odot}$, $3.71 \pm 0.03 M_{\odot}$ and $1.64 \pm 0.02 M_{\odot}$, respectively. The respective velocity of the ejecta of the three GRB-SNe are $4.22^{+0.54}_{-0.61} \times 10^9 \text{ cm s}^{-1}$, $2.61 \pm 0.02 \times 10^9 \text{ cm s}^{-1}$, and $2.17 \pm 0.03 \times 10^9 \text{ cm s}^{-1}$. The parameters are roughly consistent with the parameter ranges in the literature.

3. DISCUSSION

Here, we compare the values of the ^{56}Ni masses, the ejecta masses, the ejecta velocity, and the kinetic energy of the ejecta of the three GRB-SNe to that in the literature and discuss the reasons causing the discrepancies. Moreover, we discuss the theoretical bolometric light curves of the three GRB-SNe.

3.1. The ^{56}Ni Masses of the Three GRB-SNe

The ^{56}Ni mass of GRB 011121/SN 2001ke is $0.46 \pm 0.01 M_{\odot}$, we do not find the literature's value. The ^{56}Ni mass of GRB 130702A/SN 2013dx is $0.74 \pm 0.01 M_{\odot}$, which is ~ 2.0 and ~ 3.7 times those of the values derived by Toy et al. (2016) ($0.37 \pm 0.01 M_{\odot}$) and D'Elia et al. (2015) ($0.2 M_{\odot}$). The ^{56}Ni mass of GRB 161219B/SN 2016jca is $0.33 \pm 0.00 M_{\odot}$, which is $\sim 1.50^{+0.86}_{-0.40}$ and $\sim 1.22^{+0.28}_{-0.19}$ times those of the values derived by Cano et al. (2017a) ($0.22 \pm 0.08 M_{\odot}$) and Ashall et al. (2019) ($0.27 \pm 0.05 M_{\odot}$), respectively. The discrepancy might be due to the facts that Toy et al. (2016), Cano et al. (2017a) and Ashall et al. (2019) derived the ^{56}Ni masses by fitting the psuedo-bolometric light curves¹ which are dimmer than the bolometric light curves and that our blackbody multi-band fits correspond to the bolometric light curves.

¹ D'Elia et al. (2015) construct the psuedo-bolometric light curve of SN 2013dx and derive the ^{56}Ni mass by scaling the psuedo-bolometric light curve of SN 2003dh.

The ^{56}Ni mass of GRB 130702A/SN 2013dx is rather large, but comparable to the ^{56}Ni mass of SN 1998bw which is $0.4 - 0.7 M_{\odot}$ (Iwamoto et al. 1998; Nakamura et al. 2001) or $0.54^{+0.08}_{-0.07} M_{\odot}$ (Lyman et al. 2016). Therefore, we suggest that the ^{56}Ni mass is reasonable.

3.2. The Properties of the Ejecta

The ejecta mass of SN 2013dx and SN 2016jca are $3.71 \pm 0.03 M_{\odot}$ and $1.64 \pm 0.02 M_{\odot}$, which are lower than the values derive by the literature ($3.1 \pm 0.1 M_{\odot}$ (Toy et al. 2016) or $\sim 7 M_{\odot}$ (D’Elia et al. 2015) for SN 2013dx, $5.8 \pm 0.3 M_{\odot}$ (Cano et al. 2017a) or $6.5 \pm 1.5 M_{\odot}$ (Ashall et al. 2019) for SN 2016jca).

For example, Toy et al. (2016) and D’Elia et al. (2015) assume that the velocity of SN 2013dx are $2.13 \times 10^9 \text{ cm s}^{-1}$ and $\sim 2.9 \times 10^9 \text{ cm s}^{-1}$, respectively; Cano et al. (2017a) and Ashall et al. (2019) assume that the velocity of SN 2016jca are $2.97 \pm 0.15 \times 10^9 \text{ cm s}^{-1}$ and $3.5 \pm 0.7 \times 10^9 \text{ cm s}^{-1}$, respectively.

Our derived early-time photospheric velocities of SN 2013dx and SN 2016jca are $2.61 \pm 0.02 \times 10^9 \text{ cm s}^{-1}$ and $2.17 \pm 0.03 \times 10^9 \text{ cm s}^{-1}$. The former is between the two values adopted by Toy et al. (2016) ($2.13 \times 10^9 \text{ cm s}^{-1}$) and D’Elia et al. (2015) ($2.7 \times 10^9 \text{ cm s}^{-1}$); the latter is lower than those derived by Cano et al. (2017a) ($2.97 \pm 0.15 \times 10^9 \text{ cm s}^{-1}$), and Ashall et al. (2019) ($3.5 \pm 0.7 \times 10^9 \text{ cm s}^{-1}$).³

The kinetic energy ($E_k = \frac{3}{10} M_{\text{ej}} v_{\text{ph}}^2$) of the ejecta of SN 2001ke is $4.27^{+1.88}_{-1.60} \times 10^{52} \text{ erg}$. The kinetic energy of the ejecta of SN 2013dx is $1.51 \pm 0.04 \times 10^{52} \text{ erg}$, which is comparable to the value derive by Toy et al. (2016) ($8.2 \times 10^{51} \text{ erg}$) and significantly lower than the value inferred by D’Elia et al. (2015) ($3.5 \times 10^{52} \text{ erg}$). The kinetic energy of the ejecta of SN 2016jca is $4.6 \pm 0.2 \times 10^{51} \text{ erg}$, which is significantly lower than that derived by Cano et al. (2017a) ($5.1 \pm 0.8 \times 10^{52} \text{ erg}$).

3.3. The Theoretical Bolometric Light Curves

We use the derived best-fitting parameters to yield the bolometric light curves of the three GRB-SNe we study, see Figure 2. We find that the peak bolometric luminosities of SN 2001ke, SN 2013dx, and SN 2016jca are $1.37 \times 10^{43} \text{ erg s}^{-1}$, $1.92 \times 10^{43} \text{ erg s}^{-1}$ and $1.04 \times 10^{43} \text{ erg s}^{-1}$, respectively.

For comparison, the peak (psuedo-)bolometric luminosities of the three GRB-SNe derived by the literature are $6 \times 10^{42} \text{ erg s}^{-1}$ (Cano et al. 2017b), $1 \times 10^{43} \text{ erg s}^{-1}$ (Toy et al. 2016) and $6.3 \times 10^{42} \text{ erg s}^{-1}$ (Ashall et al. 2019) or $4.6 \times 10^{42} \text{ erg s}^{-1}$ (Cano et al. 2017a), respectively.

By comparing our derived peak bolometric luminosities of SN 2001ke, SN 2013dx, and SN 2016jca to their peak (psuedo-)bolometric luminosities in the literature, we find that the former are respectively 2.28, 1.92, and 1.65 (or 2.26) times that the latter.

The discrepancies of the peak luminosities of bolometric light curves we derive and those of the psuedo-bolometric light curves might be due to the fact that the latter omit the flux in UV and/or IR bands. Toy et al. (2016) construct the psuedo-bolometric light curve of SN 2013dx by integrating the flux in $g'r'i'z'yJ$ bands, more flux are neglected. Cano et al. (2017a) use the $griz$ band data to construct the psuedo-bolometric light curve of SN 2016jca, the flux might also be underestimated.

Our derived rise time of SN 2001ke and SN 2013dx are respectively 11.8 days and 13.7 days, which are respectively smaller than and comparable to the rise time of the two SNe in the literature which are ~ 17.5 days (Cano et al. 2017b) and ~ 14 days (Toy et al. 2016). Our derived rise time of SN 2016jca is 10.7 days, which is slightly larger than in the literature which is ~ 10 days (Ashall et al. 2019).

4. CONCLUSIONS

In the past two decades, a few dozen LGRBs have been confirmed to be associated with SNe Ic, most of which are SNe Ic-BL and HNe. While the kinetic energy of most GRB-SNe is ≥ 10 times that normal SNe Ic, their average peak luminosities are not significantly higher than those of SNe Ic. Therefore, the ^{56}Ni model adopted to account for the light curves of normal SNe Ic have also been used to explain the light curves of GRB-SNe. However, many studies exploring the energy sources of GRB-SNe construct the psuedo-bolometric light curves and fit them. This method might underestimate the ^{56}Ni masses needed to power the light curves of SNe.

We collected photometric data of three well-observed GRB-SNe (GRB 011121/SN 2001ke, GRB 130702A/SN 2013dx, GRB 161219B/SN 2016jca) and use the multi-band broken power law plus ^{56}Ni model to fit the multi-band light curves of

² This value is derived from the medians of the ejecta mass ($7 M_{\odot}$) and kinetic energy ($35 \times 10^{51} \text{ erg}$) provided by D’Elia et al. (2015), assuming $E_k = \frac{3}{10} M_{\text{ej}} v_{\text{ph}}^2$.

³ The SN velocities inferred from the spectra evolve (usually decrease) with the time. Toy et al. (2016) find that the spectral velocity of SN 2013dx inferred from the SiII lines at days 9.3, 11.3, 14.2, 31.3, 33.3 are 2.81, 2.52, 2.13, 1.17, and $1.08 \times 10^9 \text{ cm s}^{-1}$, respectively. D’Elia et al. (2015) find that the velocity of SN 2013dx decline from $\sim 2.7 \times 10^9 \text{ cm s}^{-1}$ at day 8 to $\sim 3.5 \times 10^8 \text{ cm s}^{-1}$ at day 40. Previous studies fitting the (psuedo-)bolometric light curves usually adopt the velocity derived from the spectra obtained around maximum light or earlier epochs.

the total flux which is the sum of those of the afterglows of the GRBs and the SNe. The multi-band model we use fit the observed multi-band data, rather than the psuedo-bolometric light curves constructed by taking some assumptions. A larger dataset can pose more stringent constraints on the physical parameters.

We find that the multi-band light curves of GRB 011121/SN 2001ke can be fitted by the model we use; the multi-band light curves of GRB 130702A/SN 2013dx and GRB 161219B/SN 2016jca can be fitted by the model (except their late-time z -band light curves). This indicates that the UV-optical-NIR SEDs of SNe associated with GRBs can be well described by the UV-absorbed blackbody model, and that our model can account for the multi-band light curves of the three GRB-SNe.

Our derived ^{56}Ni masses of SN 2013dx and SN 2016jca are $0.74 \pm 0.01 M_{\odot}$ and $0.33 \pm 0.00 M_{\odot}$, respectively. The former is about ~ 2.0 and ~ 3.7 times those of the values derived by Toy et al. (2016) and D’Elia et al. (2015), while the latter is $\sim 1.50^{+0.86}_{-0.40}$ and $\sim 1.22^{+0.28}_{-0.19}$ times those of the values derived by Cano et al. (2017a) and Ashall et al. (2019). This might be due to the fact that the constructed psuedo-bolometric light curves of SN 2013dx and SN 2016jca omit a fraction of the total flux. Therefore, we suggest that the ^{56}Ni masses of at least a fraction of GRB-SNe have been underestimated, and the multi-band ^{56}Ni model can make it possible to avoid underestimating the luminosities of SNe and therefore the ^{56}Ni masses.

The derived early-time photospheric velocities of SN 2013dx and SN 2016jca are $2.61 \pm 0.02 \times 10^9 \text{ cm s}^{-1}$ and $2.17 \pm 0.03 \times 10^9 \text{ cm s}^{-1}$, the former is between those adopted in the literature (2.13 or $2.7 \times 10^9 \text{ cm s}^{-1}$), while the latter is lower than that in the literature (2.97 or $3.5 \pm 0.15 \times 10^9 \text{ cm s}^{-1}$). The derived kinetic energy of SN 2013dx and SN 2016jca are $1.51 \pm 0.04 \times 10^{52} \text{ erg}$ and $4.6 \pm 0.2 \times 10^{51} \text{ erg}$. While the former is (significantly) lower in the literature ($8.2 \times 10^{51} \text{ erg}$ or $3.5 \times 10^{52} \text{ erg}$), the latter is significantly lower than that in the literature ($5.1 \pm 0.8 \times 10^{52} \text{ erg}$ for SN 2016jca).

Our study demonstrate the validity of the multi-band afterglow plus ^{56}Ni model for the the fits of multi-band light curves of GRB-SNe. The model can be regarded as an independent model that do not rely on the (psuedo-)bolometric light curves constructed. Although the GRB-SNe we fit have ample data at many bands, we expect that the model can also be used to the multi-band light curves of GRB-SNe observed in only one, two, or three bands at some or all epochs. For the GRB-SNe with sparse data, the multi-band model can play a key role to determine their physical properties by fitting their multi-band light curves, since constructing the (psuedo-)bolometric light curves is very difficult.

ACKNOWLEDGMENTS

We thank the anonymous referee for helpful comments and suggestions that have allowed us to improve this manuscript. This work is supported by National Natural Science Foundation of China (grants 11963001, 11851304, 11973020 (C0035736), and U1938201), the Bagui Scholars Program (LEW), the Special Funding for Guangxi Distinguished Professors (2017AD22006), and the Bagui Young Scholars Program (LHJ).

Table 1. The information of GRB 011121/SN 2001ke, GRB 130702A/SN 2013dx, and GRB 161219B/SN 2016jca.

	RA.	Dec.	z	$E(B - V)_{\text{MW}}^a$	$E(B - V)_{\text{host}}$	data sources ^e
GRB 011121/SN 2001ke	11 ^h 34 ^m 29 ^s .67	-76°01'41".6	0.362	0.419	$\leq 0.08^b$	1, 2, 3, 4
GRB 130702A/SN 2013dx	14 ^h 29 ^m 14 ^s .78	+15°46'26".4	0.145	0.024	0.032 ^c	5, 6, 7
GRB 161219B/SN 2016jca	06 ^h 06 ^m 51 ^s .37	-26°47'29".7	0.1475	0.028	0.017 ± 0.012^d	8, 9, 10, 11, 12, 13, 14

^a Schlafly & Finkbeiner (2011).^b Küpcü Yoldaş et al. (2007).^c Toy et al. (2016) (assuming that the value of the total to selective extinction ratio (R_V) is 3.1, which is the typical value of R_V of the Milky Way, Schultz & Wiemer 1975).^d Cano et al. (2017a).^e 1. Bloom et al. (2002); 2. Price et al. (2002); 3. Garnavich et al. (2003); 4. Greiner et al. (2003); 5. Toy et al. (2016); 6. Volnova et al. (2017); 7. D'Elia et al. (2015); 8. Buckley et al. (2016); 9. Mazaeva et al. (2016); 10. Martin-Carrillo et al. (2016); 11. Fujiwara et al. (2016); 12. Cano et al. (2017a); 13. Ashall et al. (2019); 14. Laskar et al. (2018) (The UVOT white (UVh) band data are not included, since UVh is not a narrow band data; however, the clear band data are included and labeled as R -band, since the two are closely approximated.)

Table 2. The AB magnitudes of the host galaxies of GRB 130702A/SN 2013dx and GRB 161219B/SN 2016jca.

Band	GRB 130702A/SN 2013dx	GRB 161219B/SN 2016jca
<i>K</i>	-	20.73 ± 0.11
<i>H</i>	-	20.73 ± 0.07
<i>J</i>	23.15 ± 0.48	20.80 ± 0.07
<i>z</i>	22.97 ± 0.18	20.67 ± 0.04
<i>I</i>	-	21.08 ± 0.08
<i>i</i>	22.96 ± 0.09	20.86 ± 0.03
<i>R</i>	23.17 ± 0.06	21.33 ± 0.11
<i>r</i>	23.05 ± 0.06	21.13 ± 0.05
<i>V</i>	-	21.03 ± 0.06
<i>g</i>	23.52 ± 0.06	21.48 ± 0.03
<i>B</i>	23.39 ± 0.20	$21.63^{+0.01}_{-0.05}$
<i>u</i>	-	$22.79^{+0.31}_{-0.23}$
<i>UVU</i>	-	22.62 ± 0.12
<i>UVW1</i>	-	22.95 ± 0.12
<i>UVM2</i>	-	$23.77^{+0.49}_{-0.29}$
<i>UVW2</i>	-	23.41 ± 0.23

Table 3. The definitions, the units and the prior ranges of the parameters of model.

Parameters	Definitions	Unit	Prior
A	Parameters describing the intensity of afterglow		$[10^1, 10^{40}]$
α_1	The prebreak decay slope of the afterglow light curve		$[0.01, 6]^a$
α_2	The postbreak decay slope of the afterglow light curve		$[0.01, 6]^a$
n	The sharpness of the break		$[1, 30]$
t_b	The break time	days	$[0.005, 30]^a$
β	Power-law Spectral index		$[0.01, 4]$
M_{ej}	The ejecta mass	M_\odot	$[1, 15]$
v_{ph}	The early-time photospheric velocity	10^9 cm s^{-1}	$[1.5, 5.0]$
M_{Ni}	The ^{56}Ni mass	M_\odot	$[0.1, 0.8]$
κ_γ	Gamma-ray opacity of ^{56}Ni -cascade-decay photons	$\text{cm}^2 \text{g}^{-1}$	$[10^{-1.57}, 10^3]$
T_f	The temperature floor of the photosphere	10^3 K	$[1, 15]$
$A_{V,host}$	The extinction of host galaxy	mag	$[0, 0.248]^b$

^a Based on the fits of Greiner et al. (2003), the ranges of α_1 , α_2 , and t_b of the afterglow of GRB 011121 are set to be $[0.5, 2.5]$, $[2.0, 4.0]$, and $[0.6, 1.8]$, respectively.

^b This is the range of $A_{V,host}$ of GRB 011121/SN 2001ke, the values $A_{V,host}$ of GRB 130702A/SN 2013dx and GRB 161219B/SN 2016jca are constants.

Table 4. The Best-fitting Parameters of multi-band light curves of GRB 011121/SN 2001ke, GRB 130702A/SN 2013dx, and GRB 161219B/SN 2016jca.

Parameters	GRB 011121/SN 2001ke	GRB 130702A/SN 2013dx	GRB 161219B/SN 2016jca	GRB 161219B/SN 2016jca
$\log A$	$12.74^{+0.13}_{-0.16}$	$4.67^{+0.42}_{-0.41}$	$7.36^{+0.11}_{-0.11}$	$6.70^{+0.11}_{-0.11}$
α_1	$1.71^{+0.02}_{-0.02}$	$0.48^{+0.04}_{-0.05}$	$0.19^{+0.02}_{-0.02}$	$0.01^{+0.01}_{-0.00}$
α_2	$2.28^{+0.06}_{-0.05}$	$1.64^{+0.07}_{-0.07}$	$0.77^{+0.01}_{-0.01}$	$0.77^{+0.01}_{-0.01}$
$\alpha_{2,u}$	-	-	-	$0.83^{+0.03}_{-0.03}$
$\alpha_{2,UUU}$	-	-	-	$0.89^{+0.02}_{-0.02}$
$\alpha_{2,UUV1}$	-	-	-	$0.99^{+0.02}_{-0.02}$
$\alpha_{2,UUV2}$	-	-	-	$1.03^{+0.02}_{-0.02}$
$\alpha_{2,UVM2}$	-	-	-	$0.96^{+0.02}_{-0.02}$
n	$23.49^{+4.62}_{-6.69}$	$1.03^{+0.05}_{-0.02}$	$1.96^{+0.32}_{-0.27}$	$1.17^{+0.06}_{-0.05}$
t_b (days)	$1.05^{+0.07}_{-0.06}$	$2.06^{+0.44}_{-0.40}$	$0.15^{+0.01}_{-0.01}$	$0.07^{+0.00}_{-0.00}$
β	$0.77^{+0.01}_{-0.01}$	$0.17^{+0.03}_{-0.03}$	$0.32^{+0.01}_{-0.01}$	$0.26^{+0.01}_{-0.01}$
M_{ej} (M_{\odot})	$4.02^{+0.53}_{-0.58}$	$3.71^{+0.03}_{-0.03}$	$1.70^{+0.02}_{-0.02}$	$1.64^{+0.02}_{-0.02}$
v_{ph} (10^9 cm s $^{-1}$)	$4.22^{+0.54}_{-0.61}$	$2.61^{+0.02}_{-0.02}$	$2.26^{+0.03}_{-0.03}$	$2.17^{+0.03}_{-0.03}$
M_{Ni} (M_{\odot})	$0.46^{+0.01}_{-0.01}$	$0.74^{+0.01}_{-0.01}$	$0.34^{+0.00}_{-0.00}$	$0.33^{+0.00}_{-0.00}$
$\log \kappa_{\gamma}$	$-0.79^{+0.06}_{-0.07}$	$-1.57^{+0.01}_{-0.00}$	$-1.25^{+0.03}_{-0.03}$	$-1.26^{+0.03}_{-0.03}$
T_f (10^3 K)	$8.03^{+0.11}_{-0.11}$	$5.71^{+0.04}_{-0.04}$	$4.91^{+0.12}_{-0.09}$	$4.84^{+0.09}_{-0.13}$
$A_{V,host}$ (mag)	$0.01^{+0.01}_{-0.01}$	-	-	-
χ^2/dof	6.74	13.86	13.57	12.38

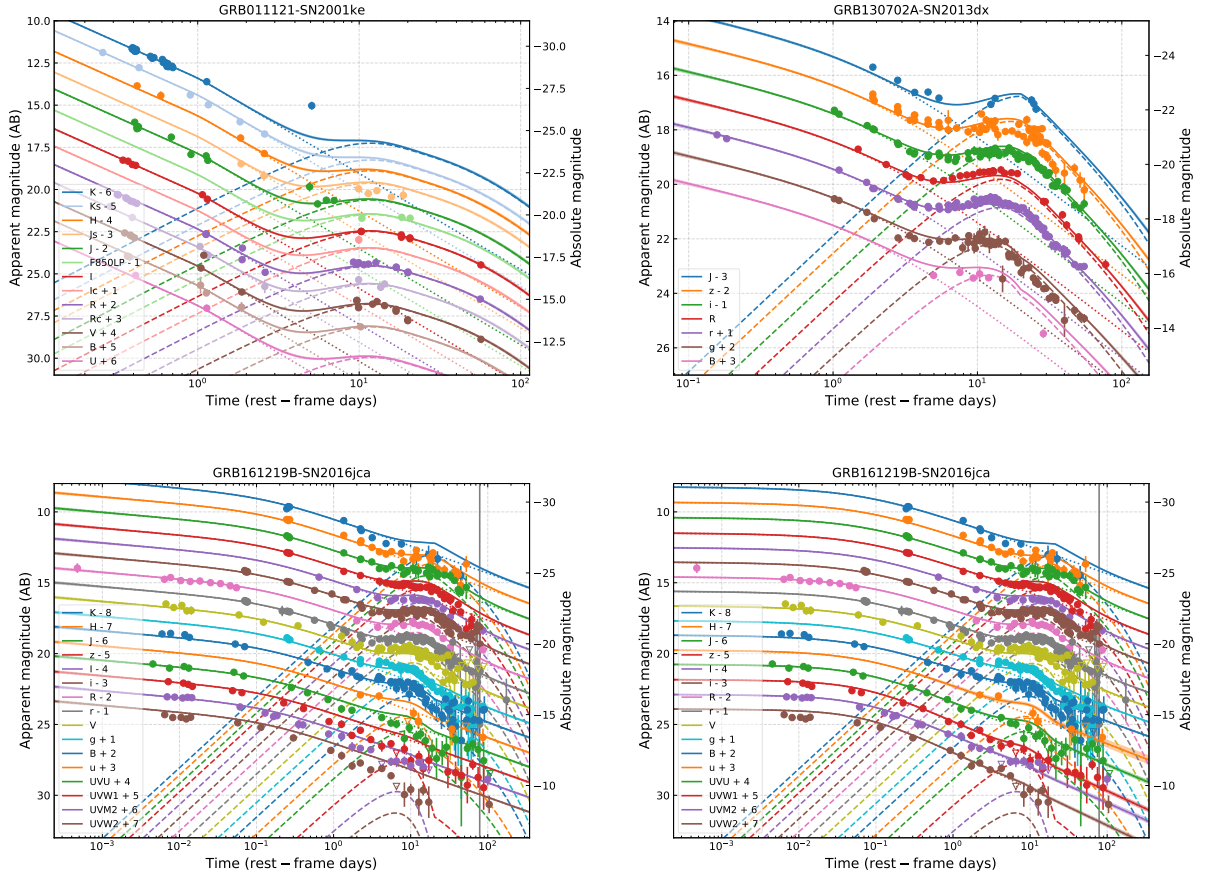


Figure 1. The fits of the multi-band light curves of GRB 011121/SN 2001ke (the top-left panel), GRB 130702A/SN 2013dx (the top-right panel) and GRB 161219B–SN 2016jca (the bottom panels). The fit represented in the bottom-left panel based on the assumption that the values of α_2 in all bands are the same one. In contrast, the fit represented in the bottom-right panel assumes that the values of α_2 in optical-NIR bands and UV bands are different, and the α_2 of UV bands are different from each other. The solid, dotted and the dashed lines represent the total flux, the afterglow flux, and the SN flux, respectively.

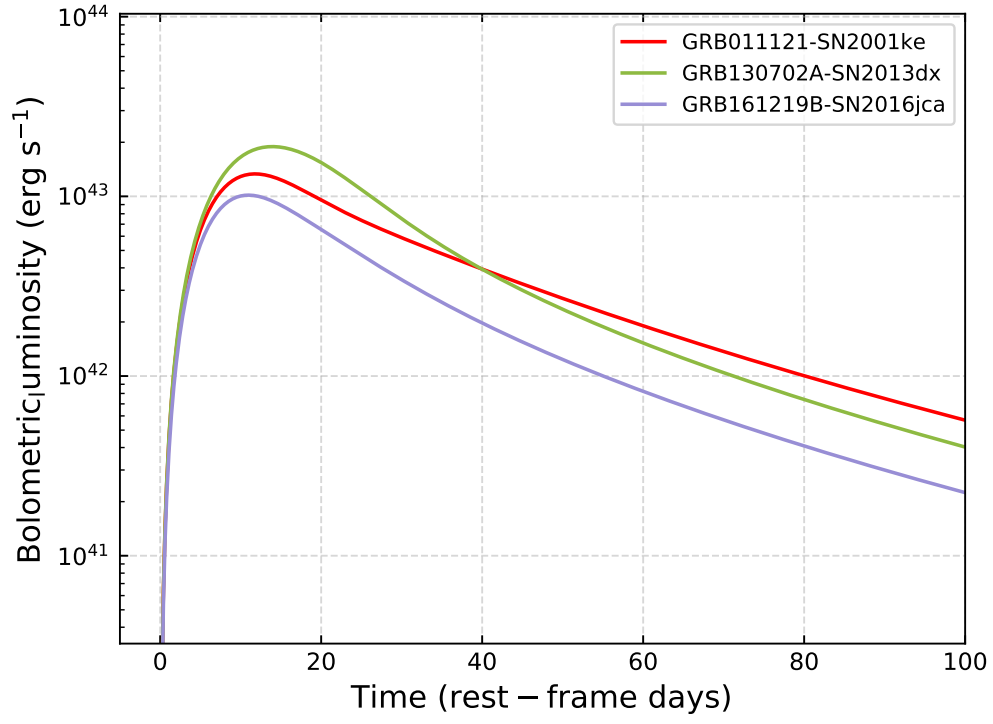


Figure 2. The bolometric light curves reproduced by the best-fitting parameters of the ^{56}Ni model.

APPENDIX

Figures A1, A2, A3, and A4 show the corner plots of the model for GRB 011121/SN 2001ke, GRB 130702A/SN 2013dx, and GRB 161219B/SN 2016jca (two cases) in the main text.

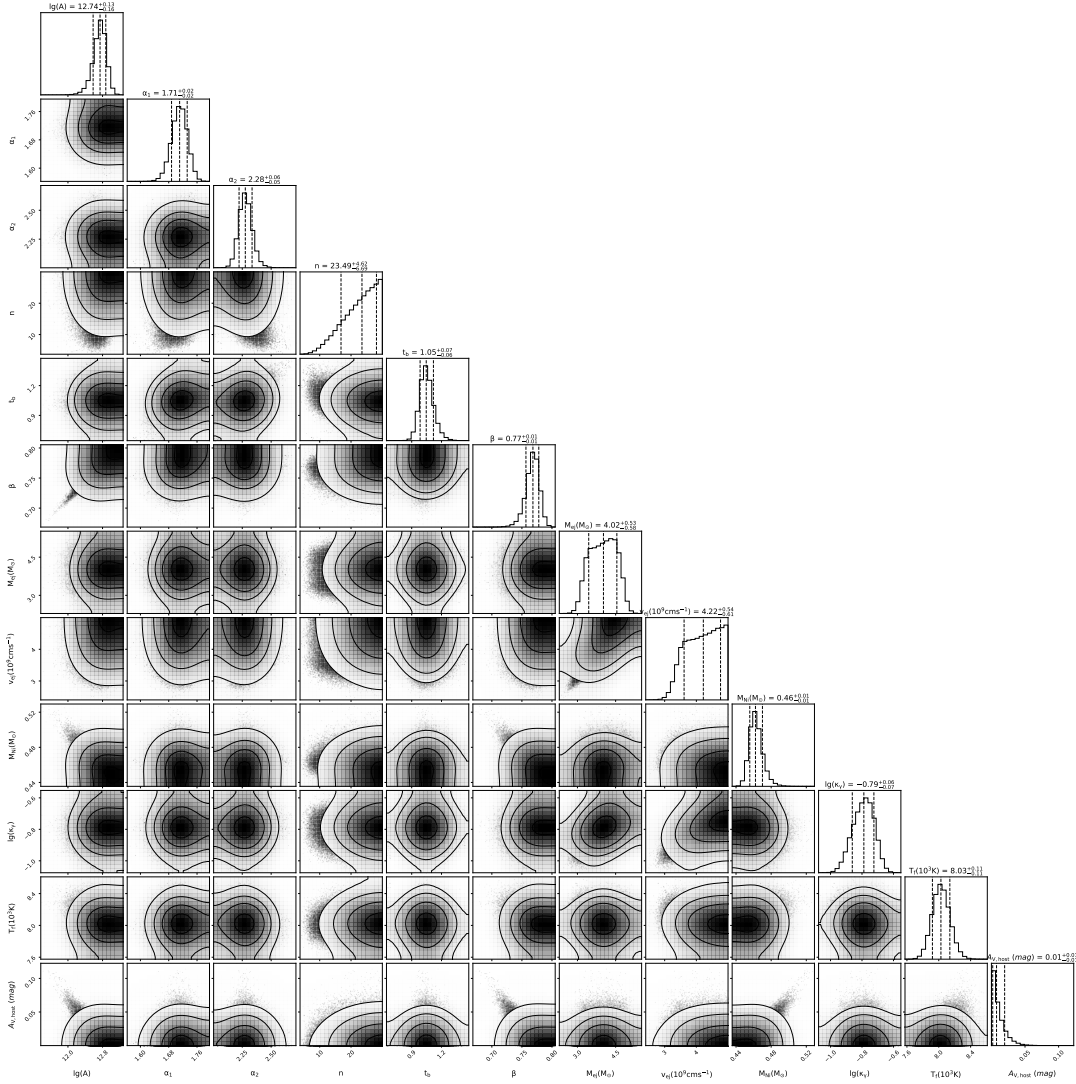


Figure A1. The corner plots of the ^{56}Ni model for multi-band light curves of GRB 011121/SN 2001ke.

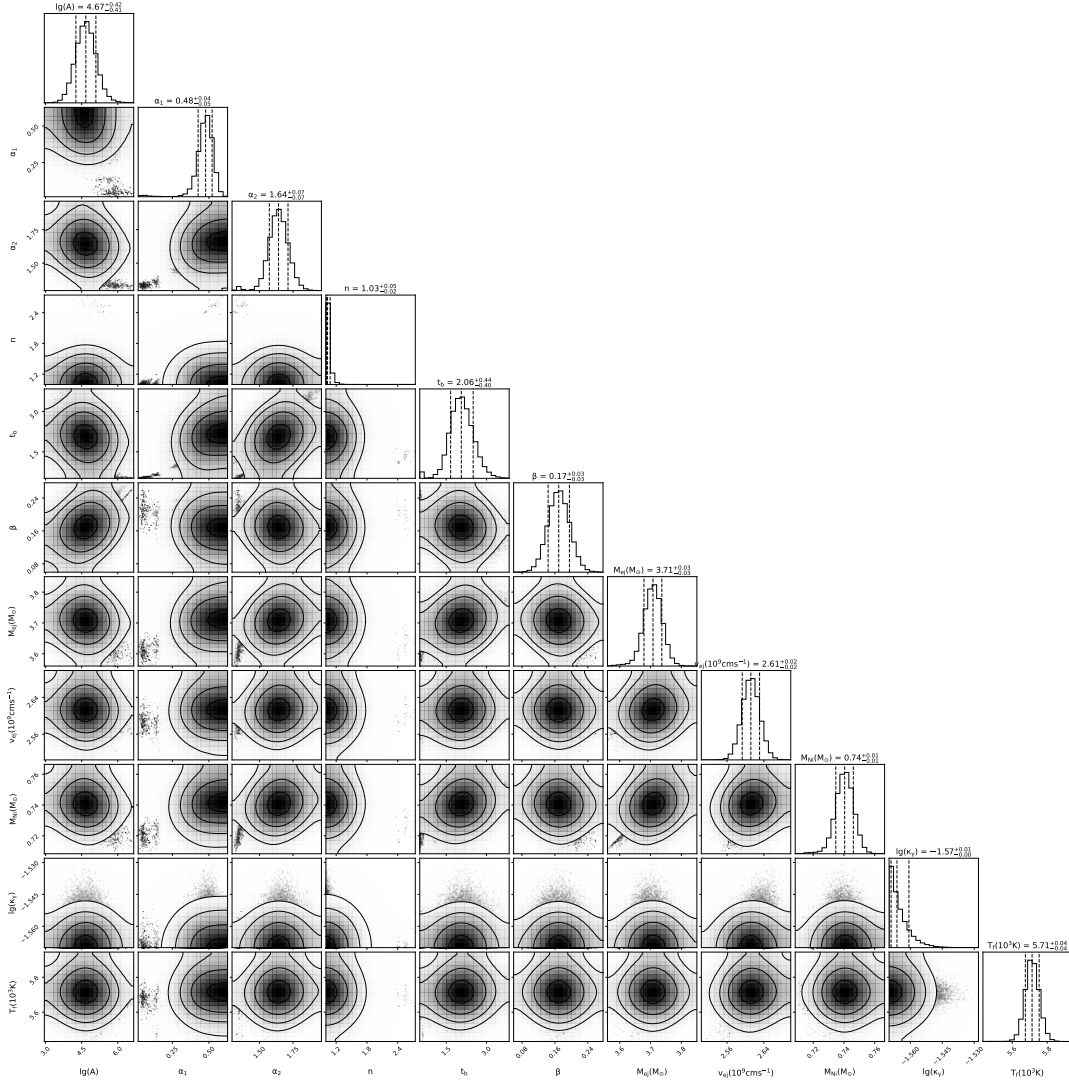


Figure A2. The corner plots of the ^{56}Ni model for multi-band light curves of GRB 130702A/SN 2013dx.

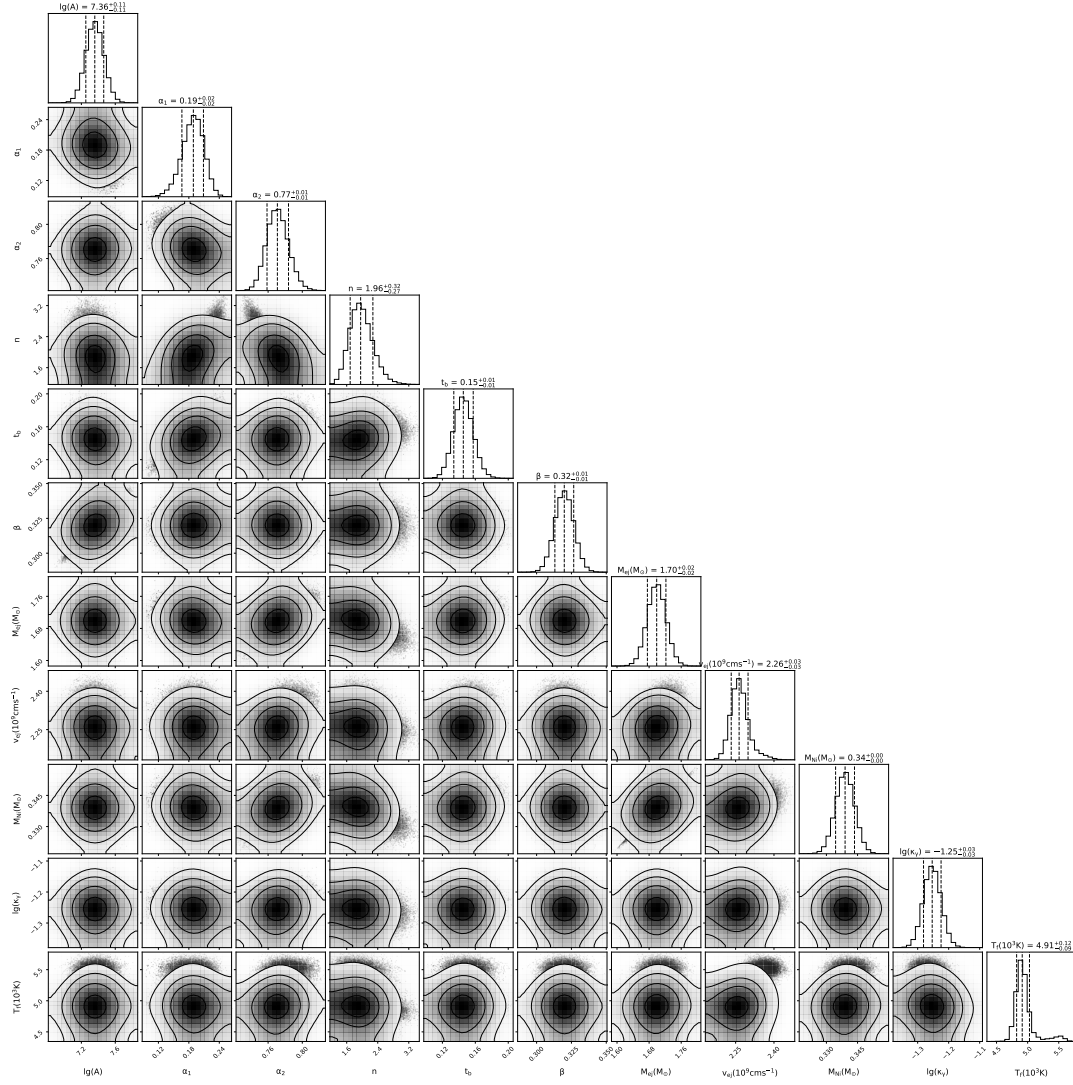


Figure A3. The corner plots of the ^{56}Ni model for multi-band light curves of GRB 161219B/SN 2016jca.

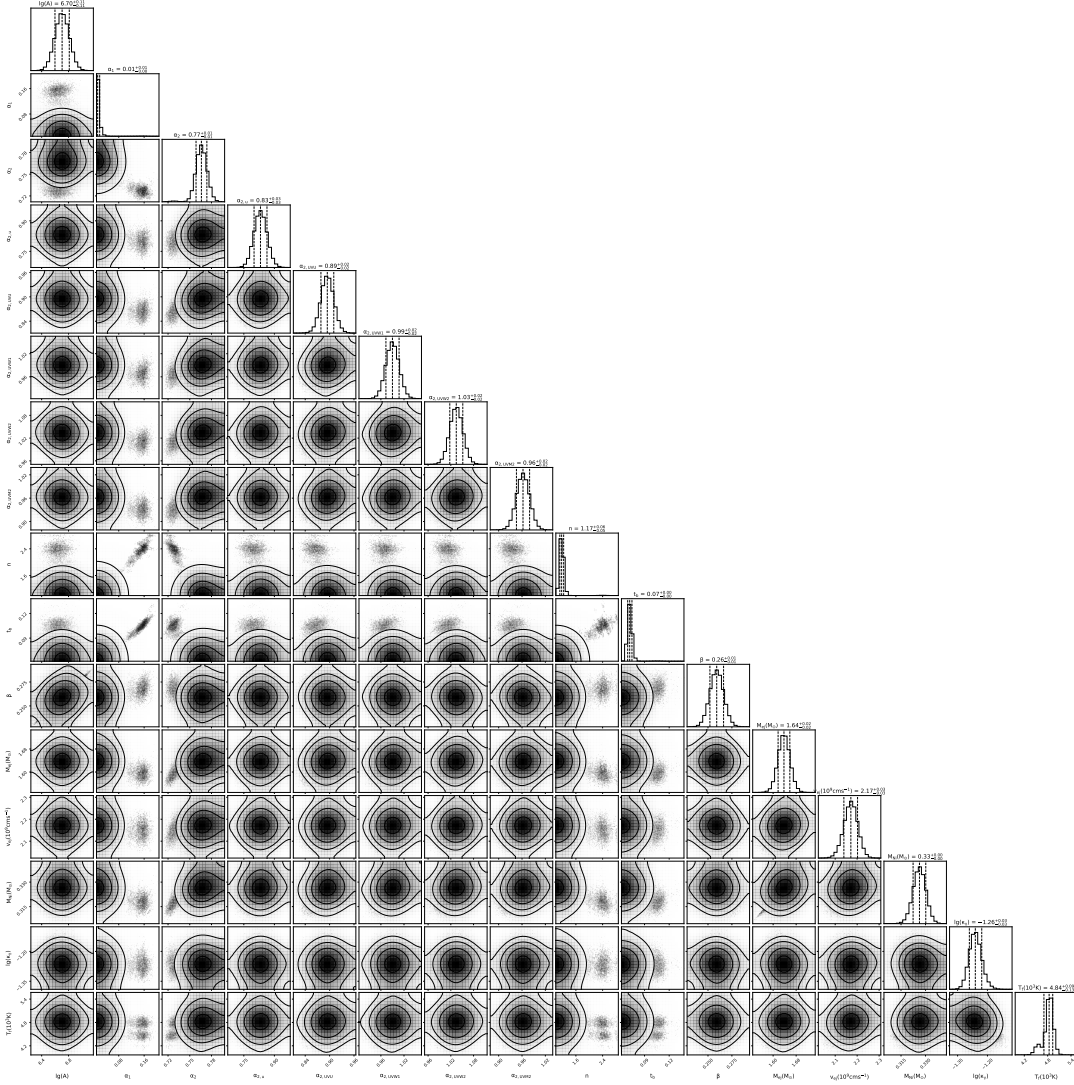


Figure A4. The corner plots of the ^{56}Ni model for multi-band light curves of GRB 161219B/SN 2016jca (assuming that the α_2 values in UV bands are different from each other, and different from that in optical and NIR bands).

REFERENCES

- Abbott, B. P., Abbott, R., Abbott, T. D., et al. 2017, *PhRvL*, 119, 1101
- Arcavi, I., Hosseinzadeh, G., Howell, D. A., et al. 2017, *Nature*, 551, 64
- Arnett, W. D. 1979, *ApJL*, 230, L37
- Arnett, W. D. 1980, *ApJ*, 237, 541
- Arnett, W. D. 1982, *ApJ*, 253, 785
- Arnett, David 1996, *Supernovae and Nucleosynthesis: An Investigation of the History of Matter from the Big Bang to the Present*
- Ashall, C., Mazzali, P. A., Pian, E., et al. 2019, *MNRAS*, 487, 5824
- Beuermann, K., Hessman, F. V., Reinsch, K., et al. 1999, *A&A*, 352, L26
- Bloom, J. S., Kulkarni, S. R., Price, P. A., et al. 2002, *ApJL*, 572, L45
- Buckley, D., Potter, S., Kniazev, A., et al. 2016, *GCN*, 20330
- Bufano, F., Pian, E., Sollerman, J., et al. 2012, *ApJ*, 753, 67
- Campana, S., Mangano, V., Blustin, A. J., et al. 2006, *Nature.*, 442, 1008
- Cano, Z., Bersier, D., Guidorzi, C., Kobayashi, S., et al. 2011, *ApJ*, 740, 41
- Cano, Z., Izzo, L., de Ugarte Postigo, A., et al. 2017a, *A&A*, 605, A107
- Cano, Z., Wang, S. Q., Dai, Z. G. & and Wu, X. F. 2017b, *Advances in Astronomy*, 8929054
- Cappellaro, E., Mazzali, P. A., Benetti, S., et al. 1997, *A&A*, 328, 203
- Chatzopoulos, E., Wheeler, J. C., & Vinko, J. 2009, *ApJ*, 704, 1251
- Chatzopoulos, E., Wheeler, J. C., & Vinko, J. 2012, *ApJ*, 746, 121
- Chornock, R., Berger, E., Levesque, et al. 2010, *arXiv e-prints*, 1004, 2262
- Coulter, D. A., Foley, R. J., Kilpatrick, C. D., et al. 2017, *Science*, 358, 1556
- D'Elia, V., Pian, E., Melandri, A., et al. 2015, *A&A*, 577, A116
- Deng, J., Tominaga, N., Mazzali, P. A., Maeda, K., & Nomoto, K. 2005, *ApJ*, 624, 898
- Foreman-Mackey, D., Hogg, D. W., Lang, D., Goodman, J. 2013, *PASP*, 125, 306
- Fujiwara, T., Saito, Y., Tachibana, Y., et al. 2016, *GCN*, 20314
- Garnavich, P. M., Stanek, K. Z., Wyrzykowski, L., et al. 2003, *ApJ*, 582, 924
- Greiner, J., Klose, S., Salvato, M., et al. 2003, *ApJ*, 599, 1223
- Hjorth, Jens, Bloom, Joshua S. 2012, *The Gamma-Ray Burst - Supernova Connection*, 169-190
- Hjorth, J., Sollerman, J., Møller, P., et al. 2003, *Nature*, 423, 847
- Hu, Y.-D., Castro-Tirado, A. J., Kumar, A., et al. 2021 *Astronomy Astrophysics*, 413, A50
- Iwamoto, K., Mazzali, P. A., Nomoto, K., et al. 1998, *Nature*, 395, 672
- Kouveliotou, C., Meegan, C. A. Fishman, G. J., et al. 1993, *ApJL*, 413, L101
- Küpcü Yoldaş, A. , Salvato, M., & Greiner, J., et al. 2007, *A&A*, 463, 893
- Laskar, T., Alexander, K. D., Berger, E., et al. 2018, *ApJ*, 862, 94
- Lyman, J. D., Bersier, D., James, P. A., et al. 2016, *MNRAS*, 457, 328
- Maeda, K., Kawabata, K., Tanaka, M., et al. 2007, *ApJ*, 658, L5
- Melandri, A., Malesani, D. B., Izzo, L., et al. 2019, *MNRAS*, 490, 5366
- Melandri, A., Pian, E., Ferrero, P., et al. 2012, *A&A*, 547, A82
- Melandri, A., Pian, E., D'Elia, V., et al. 2014, *A&A*, 567, A29
- Maeda, K., Mazzali, P. A., Deng, J., Nomoto, K., Yoshii, Y., Tomita, H., & Kobayashi, Y. 2003, *ApJ*, 593, 931
- Malesani, D., Tagliaferri, G., Chincarini, G., et al. 2004, *ApJL*, 609, L5
- Matheson, T., Garnavich, P. M., Stanek, K. Z., et al. 2003, *ApJ*, 599, 394
- Martin-Carrillo, A., Murphy, D., Hanlon, L., et al. 2016, *GCN*, 20314
- Mazaeva, E., Mokhnatkin, A., Pozanenko, A., Volnova, A., & Molotov, I. 2016, *GCN*, 20309
- Mirabal, N., Halpern, J. P., An, D., Thorstensen, J. R., Terndrup, D. M. 2006, *ApJL*, 643, L99
- Mockler, B., Guillochon, J., Ramirez-Ruiz, E. 2019, *ApJ*, 872, 151
- Modjaz, M., Stanek, K. Z., Garnavich, P. M., et al. 2006, *ApJL*, 645, L21
- Moriya, T. J., Nicholl, M., Guillochon, J. 2018, *ApJ*, 867, 113
- Nakamura, T., Mazzali, P. A., Nomoto, K., Iwamoto, K. 2001, *ApJ*, 550, 991
- Nicholl, M., Guillochon, J., Berger, E. 2017, *ApJ*, 850, 55
- Olivares, E. F., Greiner, J., Schady, P., et al. 2012, *A&A*, 539, A76
- Planck Collaboration, Ade, P. A. R., Aghanim, N., Armitage-Caplan, C., et al. 2014, *A&A*, 571, A16
- Prajs, S., Sullivan, M., Smith, M., et al. 2017, *MNRAS*, 464, 3568
- Price, P. A. , Berger, E., Kulkarni, S. R., et al. 2002, *ApJ*, 573, 85
- Price, P. A., Berger, E., Reichart, D. E., et al. 2002, *ApJL*, 572, L51
- Schlafly, E. F., & Finkbeiner, D. P. 2011, *ApJ*, 737, 103
- Schultz, G. V., Wiemer, W. 1975, *A&A*, 43, 133
- Schulze, S., Malesani, D., Cucchiara, A., et al. 2014, *A&A*, 566, A102
- Shappee, B. J., Simon, J. D., Drout, M. R., et al. 2017, *Science*, 358, 1574
- Singer, L. P., Cenko, S. B., Kasliwal, M. M., et al. 2013, *ApJL*, 776, L34
- Sollerman, J., Jaunsen, A. O., Fynbo, J. P. U., et al. 2006, *A&A*, 454, 503
- Sonbas, E., Moskvitin, A. S., Fatkhullin, T. A., et al. 2008, *Astrophysical Bulletin*, 63, 228

- Stanek, K. Z., Matheson, T., Garnavich, P. M., 2003, *ApJL*, 591, L17
- Starling, R. L. C., Wiersema, K., Levan, A. J., et al. 2011, *MNRAS*, 411, 2792
- Sutherland, P. G., & Wheeler, J. C., 1984, *ApJ*, 280, 282
- Toy, V. L., Cenko, S. B., Silverman, J. M., et al. 2016, *ApJ*, 818, 79
- Umeda, H., & Nomoto, K. 2008, *ApJ*, 673, 1014
- Volnova, A. A., Pruzhinskaya, M. V., Pozanenko, A. S., et al. 2017, *MNRAS*, 467, 3500
- Wang, S. Q., & Gan, W. P. 2022, *ApJ*, 928, 114
- Wang, S. Q., Gan, W. P., Li, L. et al. 2019, arXiv:190409604
- Wang, S. Q., Gan, W. P., Wang, T., et al. 2022, in prep.
- Wang, S. Q., Wang, L. J., Dai, Z. G., Wu, X. F. 2015, *ApJ*, 807, 147
- Woosley, S. E., Bloom, J. S. 2006, *ARA&A*44, 507
- Woosley, S. E. 2011, arXiv:1105.4193
- Zeh, A., Klose, S., & Hartmann, D. H. 2004, *ApJ*, 609, 952
- Zhang, B. 2018, *The Physics of Gamma-Ray Bursts* (Cambridge: Cambridge Univ. Press)